2004 International Symposium on Nonlinear
Theory and its Applications (NOLTA2004)
Fukuoka, Japan, Nov. 29 - Dec. 3, 2004

Simple Chaotic Spiking Oscillators having Piecewise Constant Characteristics

Yusuke Matsuoka† and Toshimichi Saito‡

†EECE Dept, Hosei University, kajino-cho, Koganei, Tokyo, 184-8584 Japan
Email: matsuoka@nonlinear.k.hosei.ac.jp, tsaito@k.hosei.ac.jp

Abstract—This paper presents novel chaotic spiking oscillators consisting of two capacitors, two signum VCCSs one voltage-controlled switch. The circuit equation has piecewise constant vector field and piecewise linear trajectory: it is well suited for theoretical analysis. We can clarify parameters condition for generation of chaotic or periodic phenomenon. Using a simple test circuits typical phenomena can be confirmed experimentally.

1. Introduction

Synthesis and analysis of simple chaotic circuits are important for understanding interesting nonlinear phenomena and various chaotic circuits have been studied [1]-[3]. We have also studied simple autonomous chaotic circuits based on integrate-and-fire switching [4] [5]. Such circuits are referred to as chaotic spiking oscillators and relate deeply to integrate-and-fire neuron models. The circuits can be developed into pulse-coupled neural networks having various applications including image segmentation [7] [6].

This paper presents a novel class of simple chaotic spiking oscillators having piecewise constant (PWC) characteristics. The oscillator consists of two capacitors, two signum voltage-controlled current sources (VCCSs) for the PWC characteristics, and one voltage-controlled switch for integrate-and-fire dynamics. We then consider four kinds of basic switching rules which can cause for interesting chaotic or periodic phenomenon. The circuit equation has piecewise constant vector field and piecewise linear trajectory: it is well suited for theoretical analysis [8]. The embedded 1D return maps are piecewise linear and can be described explicitly. Using the map we can clarify parameters condition for generation of each phenomenon. The test circuits are implemented easily using operational transconductance amplifiers (OTAs) and typical phenomena can be confirmed experimentally.

2. Circuit models and equation

Fig. 1 shows the objective circuit models. Each circuit has two capacitors, one voltage-controlled switch S and two nonlinear voltage-controlled current sources (VCCSs). The VCCSs have signum characteristics and capacitor voltage v_1 can vibrate expansively. If switch S is open all the time, the circuit dynamics is described by Equation (1).

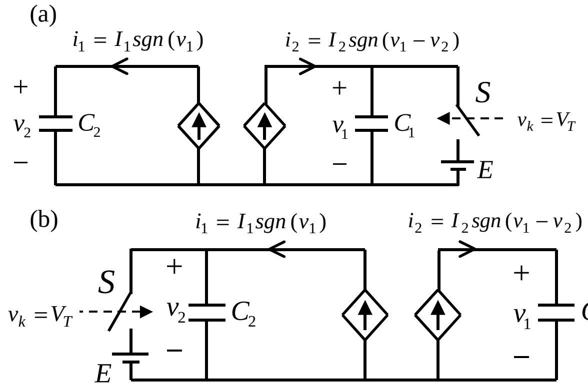

Figure 1: Circuit models

$$\begin{cases} C_1 \dfrac{dv_1}{dt} = I_2 sgn(v_1 - v_2), \\ C_2 \dfrac{dv_2}{dt} = I_1 sgn(v_1), \end{cases} \quad \text{for S=off} \tag{1}$$

$$sgn(v) = \begin{cases} 1 & \text{for } v \geq 0 \\ -1 & \text{for } v < 0. \end{cases}$$

We consider 4 switching rules. Rule A: If v_1 reaches the threshold V_T, S is closed and v_1 is reset to the base voltage E ($k = 1$ in Fig. 1 (a)). Rule B: If v_1 reaches V_T, S is closed and v_2 is reset to E ($k = 1$ in Fig. 1 (b)). Rule C: If v_2 reaches V_T, S is closed and v_2 is reset to E ($k = 2$ in Fig. 1 (b)). Rule D: If v_2 reaches V_T, S is closed and v_1 is reset to E ($k = 2$ in Fig. 1 (a)). For simplicity let the switching be instantaneous and let continuity property of opposite capacitor voltage be held. Using the following dimensionless variables and parameters for rules A and B:

$$\tau = \frac{I_2 t}{C_1 V_T}, x = \frac{v_1}{V_T}, y = \frac{v_2}{aV_T}, a = \frac{C_1 I_1}{C_2 I_2}, q_a = \frac{E}{V_T}, q_b = \frac{E}{aV_T}.$$

Equation (1) and the rules A and B are transformed into Equation (2) and Equation (3).

$$\begin{cases} \dfrac{dx}{d\tau} = sgn(x - ay), \\ \dfrac{dy}{d\tau} = sgn(x), \end{cases} \quad \text{for S= off} \tag{2}$$

$$\begin{array}{l} \text{Rule A: } (x(\tau+), y(\tau+)) = (q_a, y(\tau)) \text{ if } x(\tau) = 1 \\ \text{Rule B: } (x(\tau+), y(\tau+)) = (x(\tau), q_b) \text{ if } x(\tau) = 1 \end{array} \tag{3}$$

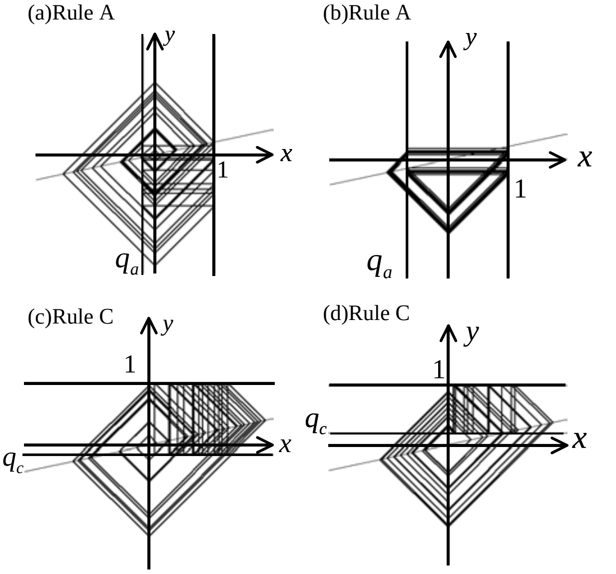

Figure 2: Typical attractors ($a = 4.7$). (a) $q_a = -0.2$, (b) $q_a = -0.68$, (c) $q_c = -0.16$, (d) $q_c = 0.2$.

Using the following dimensionless variables and parameters for rules C and D

$$\tau = \frac{I_1 t}{C_2 V_T}, x = \frac{a v_1}{V_T}, y = \frac{v_2}{V_T}, a = \frac{C_1 I_1}{C_2 I_2}, q_c = \frac{E}{V_T}, q_d = \frac{aE}{V_T}.$$

Equation (1) is transformed into Equation (2) and the rules C and D are transformed into Equation (4).

$$\begin{array}{l} \text{Rule C: } (x(\tau+), y(\tau+)) = (x(\tau), q_c) \text{ if } y(\tau) = 1 \\ \text{Rule D: } (x(\tau+), y(\tau+)) = (q_d, y(\tau)) \text{ if } y(\tau) = 1. \end{array} \quad (4)$$

It should be noted that the dimensionless system has two parameters a and q_i ($i \in \{a, b, c, d\}$) for each switching rule. For simplicity we consider the case $a > 1$ hereafter. Fig. 2 shows typical chaotic attractors by rules A and C.

3. Analysis

Rule A for $q_a < 0$: In order to derive a 1D return map, let $L = \{(x, y)|x = 0\}$ (see Fig.3) and let a point on L be represented by its y-coordinate. Since the trajectory starting from L returns to L at some positive time we can define the 1D return map f_1 from L to itself. Let y_n and y_{n+1} be the staring and return points on L, respectively. The dynamics is simplified into iteration $y_{n+1} = f_1(y_n)$. Let $Y_a \in L$ be a point such that a trajectory starting from Y_a passes the intersection of two lines $x = 1$ and $ay = x$. Let $Y_d \in L$ be a point such that the trajectory starting from Y_d hits the threshold $x = 1$ and jumps to the intersection of two lines $x = q_a$ and $ay = x$. These points are given by $Y_a = \frac{1}{a} - 1$ and $Y_d = \frac{q_a}{a} - 1$. As shown in Fig. 3 left, if $y_n \geq Y_a$ the trajectory starting from y_n returns to L without reaching the threshold $x = 1$. If $Y_a > y_n > Y_d$ (respectively, $y_n \leq Y_d$), the trajectory reaches threshold $x = 1$, jumps to the base $x = q_a$ and returns to L after intersecting (respectively, without intersecting) the line $ay = x$. Since the trajectory is piecewise linear the return map is described by

$$f_1(y_n) = \begin{cases} -\dfrac{a+1}{a-1} y_n & \text{for } y_n \geq Y_a, \\ -\dfrac{a+1}{a-1}(y_n + 1 - q_a) & \text{for } Y_a > y_n > Y_d, \\ y_n + 1 + q_a & \text{for } y_n \leq Y_d. \end{cases} \quad (5)$$

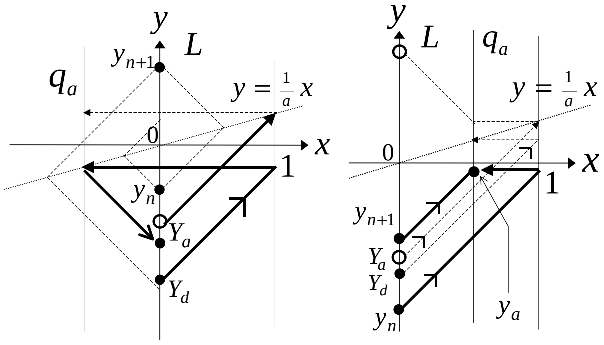

Figure 3: Phase plane for rule A

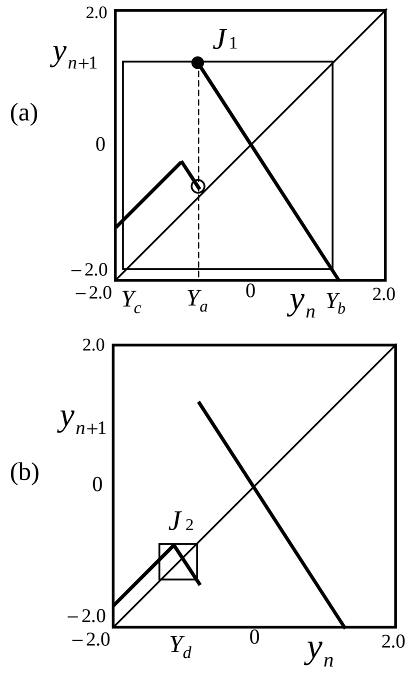

Figure 4: Return maps for rule A ($a = 4.7$). (a) $q_a = -0.2$, (b) $q_a = -0.68$.

Fig. 4 (a) and (b) show return maps corresponding to the Fig. 2 (a) and (b), respectively. Since the return map is piecewise linear, we can obtain the following results.

(R1) If $q_a < -1$ then the trajectory diverges.

(R2) Let $Y_b \equiv f_1(Y_a)$, $Y_c \equiv f_1(Y_b)$ and let $J_1 \equiv [Y_c, Y_b]$ as shown in Fig.4(a). If $0 > q_a > \frac{1-a}{1+a}$ then $f_1(J_1) \subseteq J_1$ and $|\frac{d}{dy} f_1(y_n)| \geq 1$ on J_1 are satisfied. In this case the system generates chaos [5].

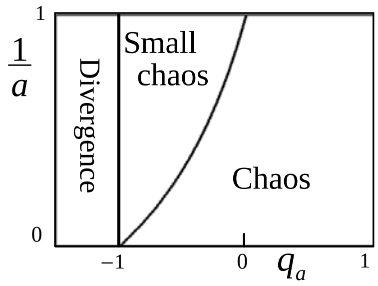

Figure 5: Parameters conditions for rule A

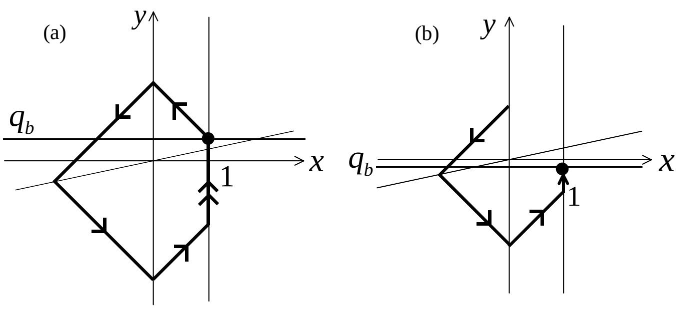

Figure 6: Trajectories for rule B. (a) $a = 4.7, \quad q_b = 0.4$, (b) $a = 4.7, \quad q_b = -0.2$.

(R3) If $\frac{1-a}{1+a} > q_a > -1$ then $f_1(Y_d) > Y_d$ and $f_1(Y_d) < Y_a$ are satisfied. In this case there exists an interval $J_2 \equiv [f_1(f_1(Y_d)), f_1(Y_d)]$ in the right-hand side of Y_a and $f_1(J_2) \subseteq J_2$ and $|\frac{d}{dy} f_1(y_n)|\,| \geq 1$ on J_2 are satisfied: chaotic attractor exists on J_2. We refer to this case as "small chaos".

Fig.5 shows parameters conditions for (R1) to (R3).

Rule A for $1 > q_a > 0$: As shown in Fig.3 definitions of Y_a, Y_d and y_n are the same as the case $q_a < 0$. For $y_n > Y_d$ we can define the 1D return map in the same manner as the case $q_a < 0$. For $y_n < Y_d$ the trajectory hits $x = 1$ and jumps to a point y_a on $x = q_a$. In this case there exists a point on L such that the trajectory starting from it passes y_a. For convenience let this point be y_{n+1}. The return map is described by Equation (6).

$$y_{n+1} = f_2(y_n) = \begin{cases} -\dfrac{a+1}{a-1} y_n & \text{for } y_n \geq Y_a \\ y_n + 1 + q_a & \text{for } Y_a > y_n > Y_d, \\ y_n + 1 - q_a & \text{for } y_n \leq Y_d. \end{cases} \quad (6)$$

This map can generate chaos for $a > 1$ and $0 < q_a < 1$ (only (R2) is satisfied).

Rule B: Fig. 6 shows trajectories by rule B. If $q_b \geq \frac{1}{a}$ the trajectory jumps to the certain point $(1, q_b)$ whenever it reaches the threshold $x = 1$ as shown in Fig. 6 (a). The system exhibits periodic attractor. If $q_b < \frac{1}{a}$ the trajectory can not move if it reaches $x = 1$ and jumps to $(1, q_b)$. This is the impasse point on the base line.

Rule C: System behavior for rule C is similar to rule A as suggested in Fig. 2. Let $M = \{(x, y) | y = 0\}$ and let point on M be represented by x-coordinate. Let $X_a \in M$ be a point such that the trajectory starting from X_a passes the intersection of two lines $y = 1$ and $x = 0$. Let $X_d \in M$ be a point such that the trajectory starting from X_d reaches the threshold $y = 1$ and jumps to the intersection of two lines $y = q_c$ and $y = \frac{1}{a}x$. These points are given by $X_a = \frac{a-1}{a+1}$ and $X_d = \frac{(a-1)(aq_c+1)}{a+1}$. In a likewise manner as rule A, we can define the 1D return map from M to itself. For $q_c < 0$ the map is described by

$$x_{n+1} = g_1(x_n) = \begin{cases} -\dfrac{a+1}{a-1} x_n & \text{for } x_n \leq X_a \\ \dfrac{a+1}{a-1} x_n - 1 - q_c & \text{for } x_n > X_a \end{cases} \quad (7)$$

For $1 > q_c > 0$ the map is described by

$$x_{n+1} = g_2(x_n) = \begin{cases} -\dfrac{a+1}{a-1} x_n & \text{for } x_n \leq X_a \\ \dfrac{a-1}{a+1}(q_c - 1) + x_n & \text{for } X_a < x_n < X_d \\ \dfrac{a+1}{a-1} x_n - 1 - q_c & \text{for } x_n \geq X_d \end{cases} \quad (8)$$

Fig. 7 (a) and (b) show return maps corresponding to Fig.2 (c) and (d), respectively. Then we have

(R4) If $q_c < \frac{a+1}{a-1}(\frac{a+1}{a-1} - 1) - 1$, the trajectory diverges.

(R5) If $q_c > \frac{a+1}{a-1}(\frac{a+1}{a-1} - 1) - 1$, the system exhibits chaos.

Fig.8 shows parameters conditions for (R4) and (R5).

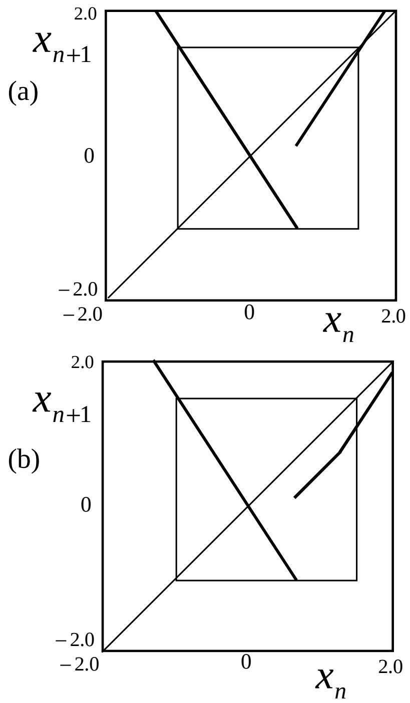

Figure 7: Return maps at switching rule C ($a = 4.7$) (a)$q_c = -0.16$, (b)$q_c = 0.2$.

Rule D: Fig. 9 shows trajectories for rule D. Behavior in this case is similar to rule B and can be summarized as the following: If $q_d \leq 0$ then the system exhibits periodic

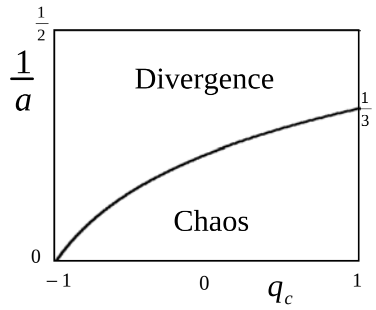

Figure 8: Parameters conditions for rule C

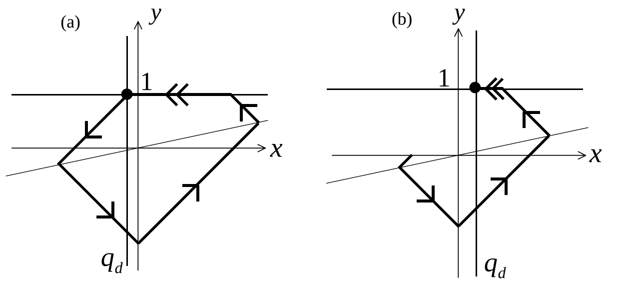

Figure 9: Trajectories for rule D. (a)$a = 4.7, \quad q_d = -0.2$, (b)$a = 4.7, \quad q_d = 0.3$

attractor passing through the point $(q_d, 1)$, and if $q_d > 0$ then the point $(q_d, 1)$ is to be the impasse point.

4. Experiments

Fig.10 shows an implementation circuit for rule A where VCCSs are realized by OTAs. If capacitor voltage $v_1(t)$ reaches the threshold V_T, the comparator (COMP) triggers the monstable multivibrator (MM) to output pulse signal that controls the switch S and $v_1(t)$ is reset to the base voltage E. The other switching rules can be implemented in a likewise manner. Fig. 11 shows the typical attractors confirmed experimentally.

5. Conclusions

We have studied simple spiking oscillators having various periodic and chaotic phenomena. The vector field is piecewise constant, the trajectory is piecewise linear and the return map is also piecewise linear. Using the return map, we have clarified parameters conditions for generation of each phenomenon. Typical phenomena are confirmed experimentally. Future problems include analysis of generalized systems, analysis of pulse-coupled systems, and consideration of engineering applications.

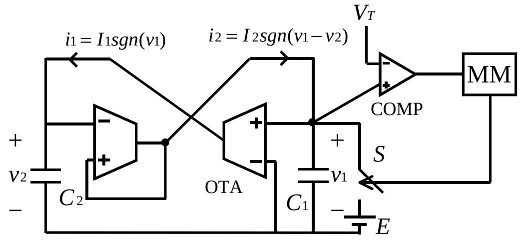

Figure 10: Implement circuit of switching rule A. $V_T = 0.5$V, $I_1 = I_2 \doteq 0.07$mA, $C_1 \doteq 47$nF, $C_2 \doteq 10$nF.

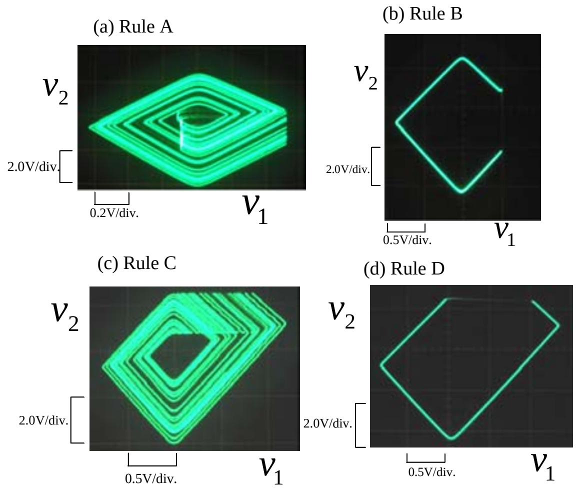

Figure 11: Laboratory experiments $a = 4.7$. (a) $E = -0.1$V ($q_a = -0.2$), (b) $E = 0.94$V ($q_b = 0.4$), (c) $E = 0.5$V($q_c = 0.2$), (d) $E = -0.1$V($q_d = -0.2$).

References

[1] G. M. Maggio, M. D. Bernardo, and M. P. Kennedy, "Nonsmooth Bifurcations in a Piecewise-Linear Model of the Colpitts Oscillator, " IEEE Trans. Circuits Syst. I, vol. 47, pp. 1160-1177, 2000.

[2] A. S. Elwakil and M. P. Kennedy, "Construction of Classes of Circuit-Independent Chaotic Oscillators Using Passive-Only Nonlinear Devices, " IEEE Trans. Circuits Syst. I, vol. 48, pp. 289-307, 2001.

[3] N. F. Rulkov and A. R. Volkovskii, "Generation of Broad-Band Chaos Using Blocking Oscillator, " IEEE Trans. Circuits Syst. I, vol. 48, pp. 673-679, 2001.

[4] K. Mitsubori and T. Saito, "Mutually Pulse-Coupled Chaotic Circuits by Using Dependent Switched Capacitors, " IEEE Trans. Circuits Syst. I, vol. 47, pp. 1469-1478, 2000.

[5] H. Nakano and T. Saito, "Basic Dynamics From a Pulse-Coupled Network of Autonomous Integrate-and-Fire Chaotic Circuits, " IEEE Trans. Neural Networks, vol. 13, pp. 92-100, 2002.

[6] H. Nakano and T. Saito, "Grouping synchronization in a pulse-coupled network of chaotic spiking oscillators, " IEEE Trans. Neural Networks, vol. 15, 2002, to appear.

[7] S. R. Campbell, D. Wang, and C. Jayaprakash, "Synchrony and desynchrony in integrate-and-fire oscillators, " Neural Comput., vol. 11, pp. 1595-1619, 1999.

[8] T. Tsubone, K. Hoshino and T. Saito, "Bifurcation from A 3-D Hysteresis Piecewise-Constant Circuit, " Proc. of IEEE / ISCAS, Sydney, III, pp. 815-818, 2001.